

# Characterization of the complete chloroplast genome of *Talinum paniculatum* (Jacq.) Gaertn. (Talinaceae) collected in Vietnam and its relatives

Thi Kim Anh Ngo<sup>1</sup> and Viet The Ho<sup>1\*</sup>

<sup>1</sup>Ho Chi Minh City University of Industry and Trade, Faculty of Biology and Environment, Ho Chi Minh city 700000, Vietnam.

\*Corresponding author (thehv@huit.edu.vn).

Received: 15 November 2025; Accepted: 3 March 2026, doi:10.4067/S0718-58392026000300449

## ABSTRACT

*Talinum paniculatum* (Jacq.) Gaertn. is an important medicinal and leafy vegetable widely used in Vietnam, yet no plastome data from Vietnamese populations have been available to support species authentication, conservation, or breeding. Here, we assembled and analyzed the complete chloroplast genome of *T. paniculatum* collected in southern Vietnam. The plastome is 156 929 bp and exhibits a typical quadripartite structure, comprising an 86 556 bp large single copy (LSC), an 18 230 bp small single copy (SSC), and two inverted repeats (IRs) of 26 071 bp. A total of 129 genes were identified, including 84 protein-coding genes, 37 tRNAs, and eight rRNAs, with 19 genes containing introns. Codon usage analysis revealed a pronounced AT bias, and 348 simple sequence repeats (SSRs) were detected, mostly A/T mononucleotides. Comparative genomics showed > 99% similarity among *Talinum* plastomes, while IR boundary variation distinguished the Vietnamese plastome from previously published accessions. Phylogenomic reconstruction confirmed the monophyly of *Talinum* and clearly separated *T. paniculatum* from *T. fruticosum* (L.) Juss. This plastome provides a Vietnam-specific genomic reference that can support molecular authentication, germplasm monitoring, and the development of genetic tools for improving *T. paniculatum* cultivation and conservation in Vietnam.

**Key words:** Chloroplast genome, IR boundaries, phylogenomics, plastome, SSRs, Talinaceae.

## INTRODUCTION

*Talinum paniculatum* (Jacq.) Gaertn. is a perennial herb widely cultivated and used across tropical and subtropical regions of Asia, Africa, and the Americas. In Vietnam, the plant holds dual importance as both a medicinal resource and a leafy vegetable, valued for its adaptogenic, antioxidant, antibacterial, and nutritional properties (Tolouei et al., 2021; Lestari et al., 2023). Its phytochemical profile includes polyphenols, saponins, flavonoids, alkaloids, and essential oils, supporting its traditional use in the treatment of metabolic disorders, inflammation, and microbial infections (Menezes et al., 2021; Aini and Susilo, 2023).

Despite this significance, the taxonomy of *Talinum* remains problematic. Morphological and anatomical traits often show high environmental plasticity, leading to frequent misidentification of species (Adenegan-Alakinde and Ojo, 2020). Molecular barcoding using internal transcribed spacer (ITS), *matK*, *rbcl*, or *psbA-trnH* has improved species discrimination, but individual loci frequently lack resolution within closely related lineages (Nguyen et al., 2018; Vu and Chu, 2018).

Chloroplast genomes offer a more robust alternative for species-level identification and phylogenetic inference. Plastomes evolve relatively slowly, possess a well-conserved structure, and contain informative variations across coding and noncoding regions. These features make them powerful tools for taxonomy, biogeography, marker development, and comparative genomics (Daniell et al., 2016; Luo, 2023). Complete

plastomes of *T. paniculatum* and *T. fruticosum* from non-Vietnamese sources have been published (Liu et al., 2018), but no plastome from Vietnamese material is available. Such region-specific data are essential for germplasm authentication, preventing misidentification in medicinal markets, and supporting breeding and conservation programs.

This study aims to assemble and annotate the complete chloroplast genome of Vietnamese *T. paniculatum*, characterize its structural features, assess sequence variability and repeat composition, evaluate inverted repeats (IR) boundary variation, and reconstruct its phylogenetic relationships within Talinaceae. The generated plastome will contribute foundational genomic resources for the authentication and sustainable utilization of *T. paniculatum* in Vietnam.

## MATERIALS AND METHODS

### Plant material and DNA extraction

Fresh leaves of *Talinum paniculatum* (Jacq.) Gaertn. were collected from cultivated plants maintained at Ho Chi Minh City University of Industry and Trade (HUIT), Vietnam. Species identity was confirmed based on morphological characteristics following Phung and Pham (2021). Voucher specimens were deposited at the Herbarium of HUIT. Approximately 100 mg leaf tissue were ground in liquid nitrogen, and total genomic DNA was extracted using the Isolate II Plant DNA Kit (Biolone, London, UK) following the manufacturer's protocol. The DNA quality was assessed by 1% agarose gel electrophoresis, and concentration and purity were measured with a spectrophotometer (NanoDrop 2000, Thermo Fisher Scientific, Waltham, Massachusetts, USA) and a fluorometer (Qubit 3.0, Invitrogen, Carlsbad, California, USA).

### Library construction and sequencing

A paired-end sequencing library (insert size  $\approx$  350 bp) was prepared using the TruSeq DNA Sample Preparation Kit (Illumina, San Diego, California, USA) and sequenced on an Illumina NovaSeq 6000 platform to generate 150 bp paired-end reads. Raw data quality was evaluated with FastQC v0.11.9, and adapters and low-quality bases (Phred < 20) were trimmed using Trimmomatic v0.39. Reads shorter than 50 bp were discarded. Clean reads were deposited in the National Center for Biotechnology Information (NCBI, Bethesda, Maryland, USA) Sequence Read Archive (SRA) under accession number PRJNA1332643.

### Genome assembly and annotation

High-quality reads were assembled using a reference-guided approach. Filtered reads were mapped to the *T. paniculatum* plastome (GenBank NC\_037748) with HISAT2 v2.2.1, and the consensus sequence was polished using Pilon v1.21 (Walker et al., 2014). The final assembly was curated using the CleanSeq module of Chloroplast Genome Viewer (CPGView, Liu et al., 2023) to remove invalid characters. Annotation was performed with GeSeq (Tillich et al., 2017) and verified manually in CPGView. Gene structure and boundaries were validated, and the circular genome map was visualized using OGDRAW (Greiner et al., 2019).

### Comparative and repeat analysis

Simple sequence repeats (SSRs) were identified using MISA-web (Beier et al., 2017), applying thresholds of  $\geq$  10 for mononucleotides,  $\geq$  5 for dinucleotides,  $\geq$  4 for trinucleotides, and  $\geq$  3 for tetra-, penta-, and hexanucleotides. Inverted repeat (IR) expansions and contractions were examined with IRscope (Amiryousefi et al., 2018). Comparative genome alignments were generated using mVISTA (Shuffle-LAGAN mode) among five *Talinum* plastomes (*T. paniculatum* NC\_037748, MG710385; *T. fruticosum* NC\_067064, OK573457) accessed from NCBI GenBank.

### Codon usage analysis

Protein-coding sequences (CDSs) were extracted from the annotated plastome, and incomplete or duplicated genes were removed. Codon frequencies were calculated using custom Python scripts. Relative synonymous codon usage (RSCU) was computed following Sharp and Li (1986). An RSCU value > 1.0 indicates codon preference, while < 1.0 denotes under-representation. Codon counts and RSCU values were summarized in

Excel, and graphical visualization was performed in Python using Matplotlib v3.8 to generate a stacked bar chart of codon usage bias across amino acids.

### Phylogenetic analysis

Complete plastome sequences of five *Talinum* accessions and three Caryophyllales outgroups (*Portulaca oleracea*, *Montia fontana*, *Plumbago auriculata*) were aligned using MAFFT v7.505 (Kato and Standley, 2013). A Maximum Likelihood (ML) tree was constructed in MEGA X under the Kimura 2-parameter model, with node support evaluated via 1000 bootstrap replicates.

## RESULTS

### Plastome structure and composition

The Vietnamese *T. paniculatum* plastome is 156 929 bp and exhibits the typical quadripartite organization of angiosperms, consisting of an 86 556 bp large single copy LSC, 18 230 bp small single copy SSC, and two IRs of 26 071 bp each (Figure 1). The *T. paniculatum* plastome encodes 84 protein-coding genes divided into three functional categories: 44 related to photosynthesis, 25 to self-replication, and 15 to other metabolic or conserved functions (Table 1). The largest group includes subunits of photosystems I and II, ATP synthase, and NADH dehydrogenase. Self-replication genes comprise *rpo*, *rpl*, and *rps* families, whereas auxiliary genes such as *accD*, *clpP*, *matK*, and *ycf1-4* play essential roles in metabolism and plastid maintenance.

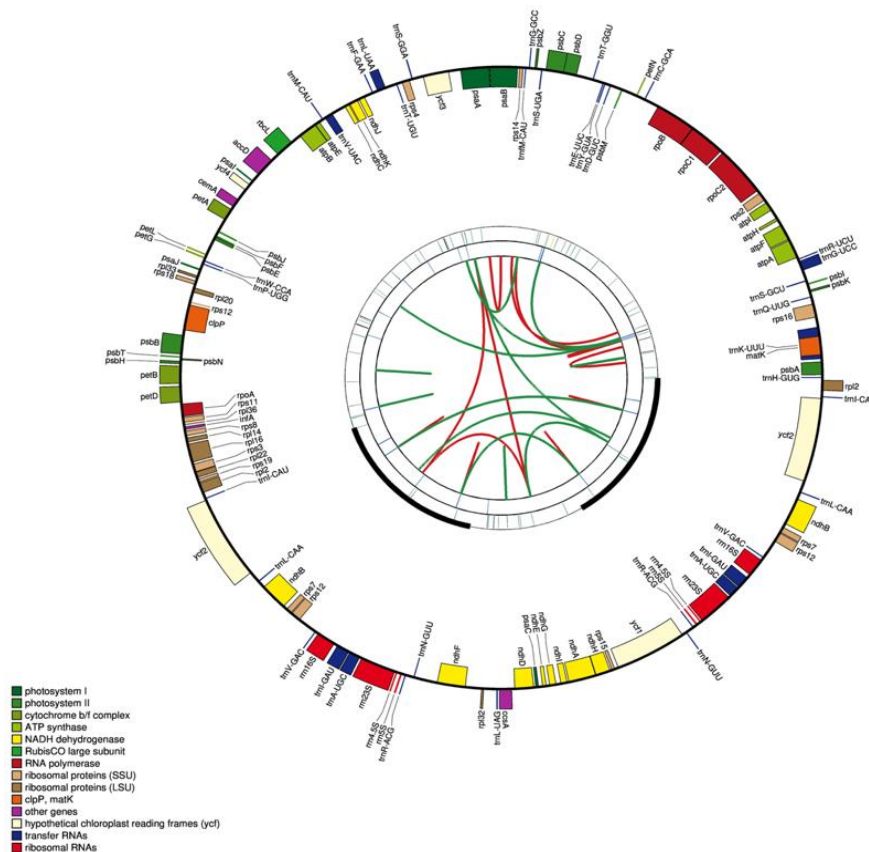


**Figure 1.** Plastome map of Vietnam *Talinum paniculatum* plastome generated using CPGView. From the center going outward, the first circle shows the forward and reverse repeats connected with red and green arcs respectively. The next circle shows the tandem repeats marked with short bars. The third circle shows the microsatellite sequences identified using MISA. The fourth circle shows the gene structure on the plastome. The genes were colored based on their functional categories.

**Table 1.** Gene composition in plastome of Vietnamese *Talinum paniculatum*.

Category of genes	Group of genes	Name of genes
Genes for photosynthesis	Subunits of ATP synthase	<i>atpA, atpB, atpE, atpF, atpH, atpI</i>
	Subunits of photosystem II	<i>psbA, psbB, psbC, psbD, psbE, psbF, psbI, psbJ, psbK, psbM, psbN, psbT, psbZ, ycf3</i>
	Subunits of NADH-dehydrogenase	<i>ndhA, ndhB(x2), ndhC, ndhD, ndhE, ndhF, ndhG, ndhH, ndhI, ndhJ, ndhK</i>
	Subunits of cytochrome b/f complex	<i>petA, petB, petD, petG, petL, petN</i>
	Subunits of photosystem I	<i>psaA, psaB, psaC, psal, psaj</i>
	Subunit of rubisco	<i>rbcl</i>
Self-replication	Large subunit of ribosome	<i>rpl14, rpl16, rpl2(x2), rpl20, rpl22, rpl32, rpl33, rpl36</i>
	DNA dependent tRNA polymerase	<i>rpoA, rpoB, rpoC1, rpoC2</i>
	Small subunit of ribosome	<i>rps11, rps12(x2), rps14, rps15, rps16, rps18, rps19, rps2, rps3, rps4, rps7(x2), rps8</i>
Other genes	Subunit of Acetyl-CoA-carboxylase	<i>accD</i>
	c-type cytochrome synthesis gene	<i>ccsA</i>
	Envelope membrane protein	<i>cemA</i>
	Protease	<i>clpP</i>
	Maturase	<i>matK</i>
	Conserved open reading frames	<i>ycf1, ycf2(x2), ycf4</i>

### Intron-exon structure

The intron-exon length analysis revealed consistent structural organization among intron-containing genes in the *T. paniculatum* plastome (Table 2). Among the 19 intron-containing genes, 17 contain a single intron, while *clpP* and *ycf3* contain two introns. The total intron lengths ranged from 586 bp (*trnV-UAC*) to 2502 bp (*trnK-UUU*), while exon lengths were generally short and conserved, averaging 40-500 bp.

**Table 2.** Lengths of introns and exons for the split genes in the plastome of Vietnamese *Talinum paniculatum*.

Gene	Strand	Start	End	Exon I	Intron I	Exon II	Intron II	Exon III
<i>trnK-UUU</i>	-	1540	4113	37	2502	35		
<i>rps16</i>	-	4907	6016	41	867	202		
<i>trnG-UCC</i>	+	8817	9594	23	707	48		
<i>atpF</i>	-	11533	12832	145	745	410		
<i>rpoC1</i>	-	20421	23257	432	794	1611		
<i>ycf3</i>	-	43352	45400	124	769	230	773	153
<i>trnL-UAA</i>	+	48444	49129	37	599	50		
<i>trnV-UAC</i>	-	53103	53761	38	586	35		
<i>clpP</i>	-	72527	74601	71	894	294	590	226
<i>petB</i>	+	77500	78915	6	768	642		
<i>petD</i>	+	79125	80399	8	792	475		
<i>rpl16</i>	-	83819	85328	9	1102	399		
<i>ndhB</i>	-	96874	99074	775	668	758		
<i>trnI-GAU</i>	+	104316	105334	37	947	35		
<i>trnA-UGC</i>	+	105405	106295	38	818	35		
<i>ndhA</i>	-	122983	125161	553	1087	539		
<i>trnA-UGC</i>	-	137533	138423	38	818	35		
<i>trnI-GAU</i>	-	138494	139512	37	947	35		
<i>ndhB</i>	+	144754	146954	775	668	758		

### Codon usage

A total of 26 622 codons were identified in protein-coding genes. Codon usage exhibited strong AT bias at the third codon position; TTA (Leu), ATT (Ile), and AAA (Lys) were the most frequently used codons. The RSCU values ranged from 0.33 to 1.91, with 30 codons showing RSCU > 1.0 (Figure 2).

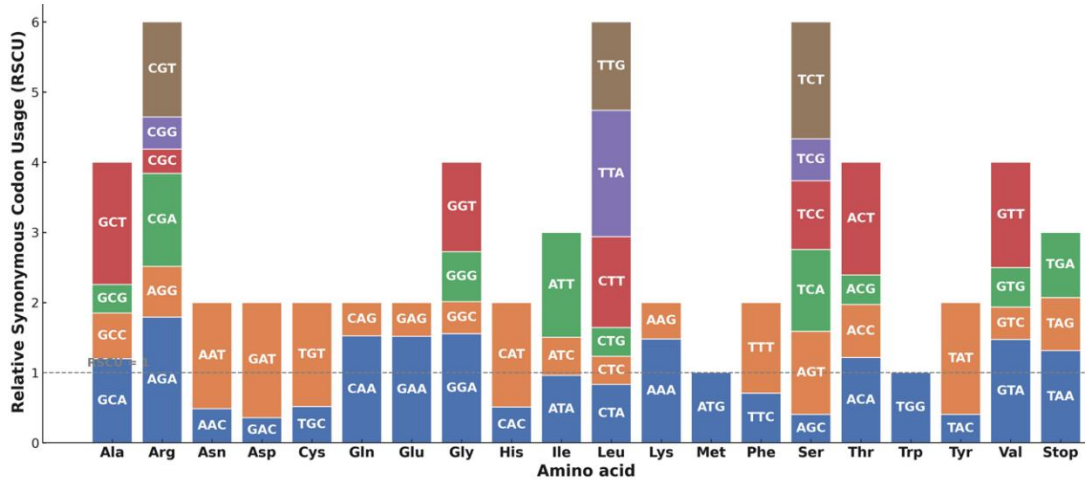


**Figure 2.** Distribution and frequency of codon usage in the plastome of *Talinum paniculatum*. Bars represent relative synonymous codon usage (RSCU) values for each codon.

### Simple sequence repeats

A total of 348 SSRs were identified revealed both conserved and minor variable patterns among accessions (Figure 3). In the Vietnamese plastome, the number of A and T mononucleotide repeats was highly conserved (33 each), while C and G repeats occurred only once. Among identified SSRs, mononucleotide motifs accounting for 91.5%. Small differences appeared in dinucleotide repeats: The Vietnamese sample carried three AT and three TA motifs, compared to two of each in other *T. paniculatum* accessions. By contrast, *T. fruticosum* exhibited a slightly higher number of A mononucleotide and dinucleotide repeats. The high frequency of A/T repeats is typical for chloroplast genomes and contributes to their AT-rich composition.

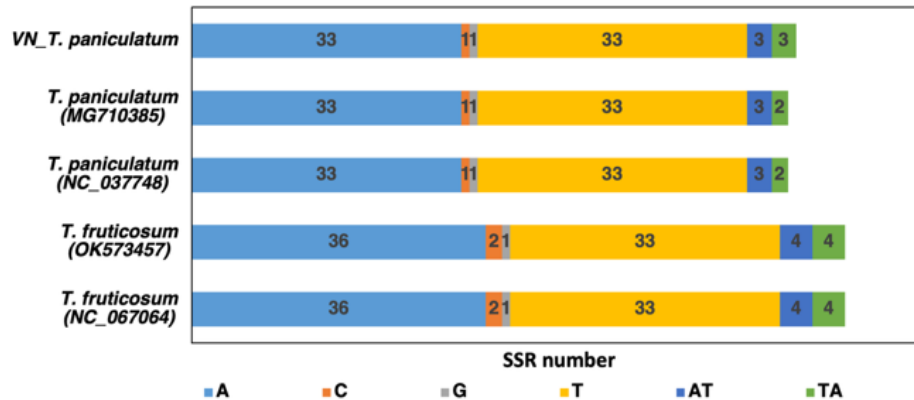


**Figure 3.** Simple sequence repeat (SSR) types identified in five *Talinum* plastomes, including the Vietnamese accession (VN\_ *T. paniculatum*).

### IR boundary comparison

Comparison of IR/single-copy (SC) boundary regions among *T. paniculatum* and *T. fruticosum* plastomes revealed overall structural conservation with only minor boundary shifts (Figure 4). The significant difference among *T. paniculatum* and *T. fruticosum* plastomes is the absence of *rps19* at the inverted repeat A (IRA)/LSC border in *T. paniculatum* plastomes. The Vietnamese plastome displayed the presence of *rps1* in place of *rps19* of two other *T. paniculatum* plastomes.

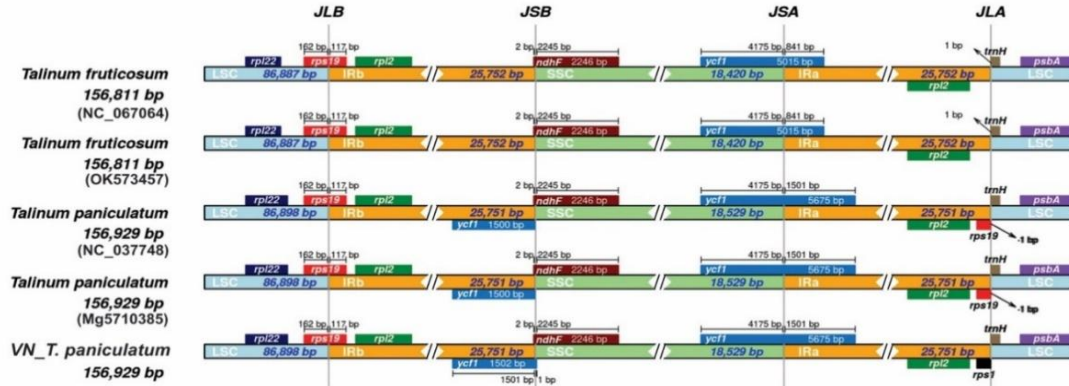


**Figure 4.** Comparison of the boundary regions (JLB, JSB, JSA, JLA) between the large single-copy (LSC), small single-copy (SSC), and inverted repeats (IRs) among five *Talinum* plastomes. Genes located at the IR/SC borders are represented by boxes above or below the main lines, with the numbers above the gene indicating the distance in bp from the gene terminal to the boundary region. VN\_*T. paniculatum*: *Talinum paniculatum* accession collected from Vietnam.

### Comparative genomics and phylogenetic relationships

The mVISTA alignment of five *Talinum* chloroplast genomes, using the Vietnamese plastome as reference, revealed high sequence conservation (Figure 5). The two *T. paniculatum* accessions from GenBank were nearly identical to the Vietnamese plastome, whereas *T. fruticosum* showed greater divergence. Maximum Likelihood analysis based on complete plastome sequences recovered *Talinum* as a well-supported monophyletic clade within Talinaceae (Figure 6). *Talinum paniculatum* accessions from different geographic origins clustered together with full bootstrap support, while *T. fruticosum* formed a sister lineage.

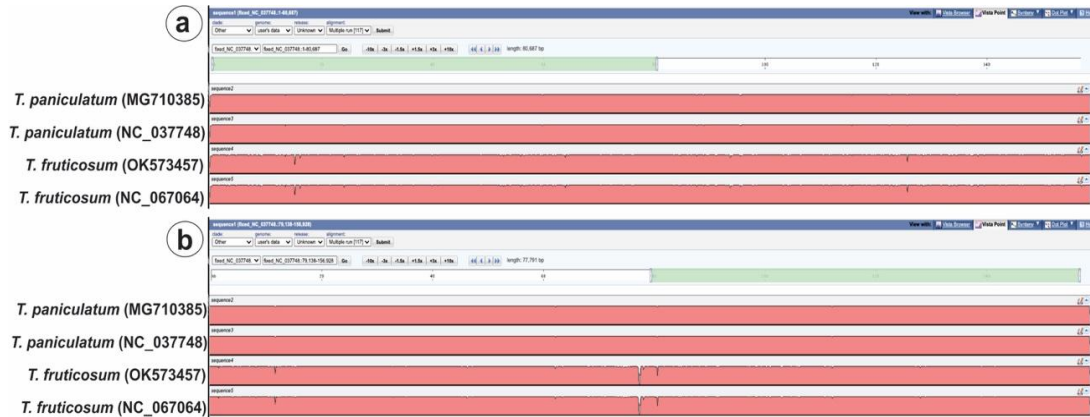


**Figure 5.** Sequence alignment of five *Talinum* plastomes using mVISTA. The Vietnamese *Talinum paniculatum* plastome is used as a reference: LSC-IRb-SSC region (a); SSC-Ira-LSC region of the plastome alignment (b). LSC: Large single copy; IRb: inverted repeat b; SSC: small single copy; Ira: inverted repeat a.

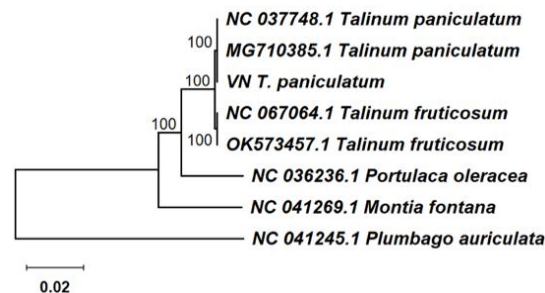


**Figure 6.** Maximum likelihood (ML) phylogenetic tree inferred from complete plastome sequences of *Talinum paniculatum*, *T. fruticosum*, and related Caryophyllales species. Bootstrap values (1000 replicates) are indicated above the branches.

## DISCUSSION

The complete chloroplast genome of *Talinum paniculatum* from Vietnam exhibits overall structural conservation compared with previously reported *Talinum* plastomes (Liu et al., 2018), yet several distinctive features highlight its regional specificity and biological relevance. These differences, including shifts at the inverted repeat A (IRa)/large single-copy (LSC) boundary, variation in noncoding divergence patterns, and differences in simple sequence repeats (SSR) abundance and distribution, underscore the importance of generating localized plastome references for species with wide ecological amplitude and extensive morphological plasticity (Adenegan-Alakinde and Ojo, 2020).

One of the most notable variations is the absence of *rps19* at the IRa/LSC junction, where the Vietnamese plastome instead positions *rps1*. Shifts in IR boundaries are widely recognized as lineage-specific signatures in angiosperm plastomes (Daniell et al., 2016; Androsiuk et al., 2020), and the deviation observed here distinguishes the Vietnamese accession from previously sequenced *T. paniculatum*. Such structural differences may reflect historical demographic processes, local adaptation, or geographic isolation. For *Talinum*, a genus where species delimitation has long been hampered by convergent morphology and environmental plasticity (Veselova et al., 2012), region-specific plastome features offer robust markers for clarifying species boundaries and evaluating intraspecific diversification.

Comparative genomic analysis also revealed enhanced variation in several intergenic regions, exceeding that reported by Liu et al. (2018). These hotspots of divergence provide candidates for developing locally informative DNA barcodes or high-resolution markers for Vietnamese populations. Traditional barcodes like ITS or *matK* often fail to resolve closely related *Talinum* species (Nguyen et al., 2018; Vu and Chu, 2018). Therefore, the variable regions identified here contribute essential molecular tools for distinguishing Vietnamese accessions from those cultivated in other regions or introduced through trade.

The Vietnamese plastome also contained a higher number of SSRs than previously documented. The SSR variation is particularly valuable because A/T-rich microsatellites evolve rapidly, offering sensitivity for detecting fine-scale population structure, hybridization events, and germplasm purity (Shen et al., 2024). These markers have direct applications in Vietnam, where *T. paniculatum* is sourced from multiple informal cultivation systems, frequently mixed with *T. fruticosum* in markets, and exploited for its medicinal properties (Menezes et al., 2021; Aini and Susilo, 2023). The SSRs from the Vietnamese genome can therefore assist in authentication of commercial materials, certification of planting stocks, and preservation of elite local varieties.

Codon usage bias in the Vietnamese plastome showed AT enrichment consistent with typical chloroplast genomes (Sharp and Li, 1986; Wang et al., 2022), but subtle shifts in relative synonymous codon usage (RSCU) values for amino acids such as leucine and serine may indicate lineage-specific mutational patterns. These patterns, while modest, contribute additional molecular characters that differentiate the Vietnamese accession from previously studied samples and may prove useful for phylogeographic or evolutionary analyses.

Phylogenomic reconstruction robustly separated *T. paniculatum* from *T. fruticosum*, reinforcing species boundaries previously supported by morphology and chemical profiles (Liu et al., 2018; Tolouei et al., 2021; Lestari et al., 2023). Importantly, the Vietnamese *T. paniculatum* formed a well-supported clade distinct from

other reported accessions, suggesting potential regional structuring within the species. This highlights the importance of incorporating Vietnamese material into broader phylogenomic frameworks and raises the possibility that overlooked diversity exists within Southeast Asian populations.

## CONCLUSIONS

Taken together, the plastome features identified in the Vietnamese sample provide genomic signatures that distinguish this accession from previously sequenced material. These differences are not only taxonomically informative but also hold substantial practical value for Vietnam. They enable the development of localized molecular markers for authentication of medicinal products, facilitate monitoring of germplasm purity in cultivation systems, and support the conservation and breeding of *Talinum paniculatum* suited to diverse agroecological zones across the country.

### Author contribution

Conceptualization: T.K.A.N., V.T.H. Methodology: T.K.A.N., V.T.H. Software: V.T.H. Validation: V.T.H. Formal analysis: T.K.A.N., V.T.H. Investigation: T.K.A.N., V.T.H. Data curation: V.T.H. Writing-original draft: T.K.A.N., V.T.H. Writing-review & editing: T.K.A.N., V.T.H. Visualization: T.K.A.N., V.T.H. Supervision: V.T.H. Project administration: T.K.A.N., V.T.H. Funding acquisition: T.K.A.N., V.T.H. All co-authors reviewed the final version and approved the manuscript before submission.

### Acknowledgements

This work was financially supported by Ho Chi Minh City University of Industry and Trade under Contract no 249/HD-DCT dated 01 July 2025.

### References

- Adenegan-Alakinde, T.A., Ojo, F.M. 2020. Comparative anatomical studies of two *Talinum* occurring in Southwestern Nigeria. *Ife Journal of Science* 22(1):75-85. doi:10.4314/ijfs.v22i1.8.
- Aini, F.N., Susilo, F. 2023. Phytochemical profiling of Javanese ginseng (*Talinum paniculatum*) stem extract using GC-MS analysis and pharmacological potential. *Tropical Journal of Natural Product Research* 7(7):3272-3278. doi:10.26538/tjnpr/v7i7.1.
- Amiryousefi, A., Hyvönen, J., Poccai, P. 2018. IRscope: an online program to visualize the junction sites of chloroplast genomes. *Bioinformatics* 34(17):3030-3031. doi:10.1093/bioinformatics/bty220.
- Androsiuk, P., Jastrzębski, J.P., Paukzto, L., Makowczenko, K., Okorski, A., Pszczolkowska, A., et al. 2020. Evolutionary dynamics of the chloroplast genome sequences of six *Colobanthis* species. *Scientific Reports* 10:11522. doi:10.1038/s41598-020-68563-5.
- Beier, S., Thiel, T., Münch, T., Scholz, U., Mascher, M. 2017. MISA-web: A web server for microsatellite prediction. *Bioinformatics* 33:2583-2585. doi:10.1093/bioinformatics/btx198.
- Daniell, H., Lin, C.-S., Yu, M., Chang, W.-J. 2016. Chloroplast genomes: Diversity, evolution, and applications in genetic engineering. *Genome Biology* 17:134. doi:10.1186/s13059-016-1004-2.
- Greiner, S., Lehwark, P., Bock, R. 2019. OrganellarGenomeDRAW (OGDRAW) version 1.3.1: expanded toolkit for the graphical visualization of organellar genomes. *Nucleic Acids Research* 47(W1):59-W64. doi:10.1093/nar/gkz238.
- Katoh, K., Standley, D.M. 2013. MAFFT multiple sequence alignment software version 7: Improvements in performance and usability. *Molecular Biology and Evolution* 30(4):772-780. doi:10.1093/molbev/mst010.
- Lestari, P.D., Fajrisani, S., Gehasti, P., Sugiharto, Manuhara, Y.S.W. 2023. Optimization of *Talinum paniculatum* root induction and the effect of phosphate concentrations and ammonium:nitrate ratio on biomass of adventitious roots in vitro. *Biotropia* 30(2):137-146. doi:10.11598/btb.2023.30.2.1678.
- Liu, X., Li, Y., Yang, H., Zhou, B. 2018. Chloroplast genome of the folk medicine and vegetable plant *Talinum paniculatum*: gene organization, comparative and phylogenetic analysis. *Molecules* 23:857. doi:10.3390/molecules23040857.
- Liu, S., Ni, Y., Li, Y., Zhang, X., Yang, H., Chen, H., et al. 2023. CPGView: A package for visualizing detailed chloroplast genome structures. *Molecular Ecology Resources* 23(3):694-704. doi:10.1111/1755-0998.13729.
- Luo, Y. 2023. Application of chloroplast genome analysis in plant taxonomy. p. 296-300. In *Proceedings of the 2<sup>nd</sup> International Conference on Modern Medicine and Global Health*, Oxford. 15 April. doi:10.54254/2753-8818/8/20240434.
- Menezes, F.D.A.B., Ishzawa, T.A., Souto, L.R.F., de Oliveira, T.F. 2021. *Talinum paniculatum* leaves: Source of nutrients, antioxidant and bacterial potentials. *Acta Scientiarum Polonorum Technologia Alimentaria* 20(3):253-263. doi:10.17306/J.AFS.0892.

- Nguyen, T.N.L., Nguyen, H.Q., Nguyen, T.H., Lo, T.M.T., Chu, H.M. 2018. Use of ITS DNA barcode for identification of Jewels of Opar (*Talinum paniculatum*) collected in Thanh Hoa, Vietnam. Vietnam Journal of Science, Technology and Engineering 60(1):46-49.
- Phung, T.T.H., Pham, T.H.T. 2021. Botanical characteristics of *Talinum paniculatum* and *Talinum fruticosum* in Gialam district, Hanoi. Vietnam Academy of Agricultural Sciences 6(127):36-42.
- Sharp, P.M., Li, W.H. 1986. An evolutionary perspective on synonymous codon usage in unicellular organisms. Journal of Molecular Evolution 24(1):28-38. doi:10.1007/BF0209994.
- Shen, L., Chen, S., Liang, M., Zhao, W., Han, J. 2024. Codon usage bias in chloroplast genomes of ten medicinal Rutaceae species. BMC Plant Biology 24:424. doi:10.1186/s12870-024-04999-5.
- Tillich, M., Lehwark, P., Pellizzer, T., Ulbricht-Jones, E.S., Fischer, A., Bock, R., et al. 2017. GeSeq – versatile and accurate annotation of organelle genomes. Nucleic Acids Research 45(W1):W6-W11. doi:10.1093/nar/gkx391.
- Tolouei, S.E.L., de Silva, G.N., Curi, T.Z., Menezes, D., and Carvalho, S. 2021. Effects of *Talinum paniculatum* leaf extract on toxicity and pubertal development of rats. Human & Experimental Toxicology 40(1):124-135. doi:10.1177/096032712094575.
- Veselova, T.D., Dzhaliilova, K.K., Remizowa, M.V., Timonin, A.C. 2012. Embryology of *Talinum paniculatum* (Jacq.) Gaertn. and *T. triangulare* (Jacq.) Willd. (Portulacaceae s.l., Caryophyllales). Wulfenia 19:107-129.
- Vu, T.N.T., Chu, H.M. 2018. Use of *matK* DNA barcode for identification of jewels of opar (*Talinum paniculatum*) samples collected at some localities in in the Northern Vietnam. Journal of Science and Technology 184(08):101-106 (In Vietnamese)
- Walker, B.J., Abeel, T., Shea, T., Priest, M., Abouelliel, A., Sakthikumar, S., et al. 2014. Pilon: An integrated tool for comprehensive microbial variant detection and genome assembly improvement. PLOS ONE 9(11):e112963. doi:10.1371/journal.pone.0112963.
- Wang, Z., Cai, Q., Wang, Y., Chen, L., Zhao, Y. 2022. Comparative analysis of codon bias in chloroplast genomes of Theaceae species. Frontiers in Genetics 13:824610. doi:10.3389/fgene.2022.824610.